Biological Journal of the Linnean Society, 2021, **132**, 829–846. With 6 figures.

Stability in the Balkans: phylogeography of the endemic Greek stream frog, *Rana graeca*

DANIEL JABLONSKI[1*], IOANNIS GKONTAS[2,3], DIMITRIS POURSANIDIS[4], PETROS LYMBERAKIS[3] and NIKOS POULAKAKIS[2,3]

[1]*Department of Zoology, Comenius University in Bratislava, Ilkovičova 6, Mlynská dolina, 842 15, Bratislava, Slovakia*
[2]*Department of Biology, School of Sciences and Engineering, University of Crete, Vassilika Vouton, Irakleio, GR70013, Greece*
[3]*Natural History Museum of Crete, School of Sciences and Engineering, University of Crete, Knosos Avenue, Irakleio, GR71409, Greece*
[4]*Foundation for Research and Technology Hellas, Institute of Applied and Computational Mathematics, The Remote Sensing Lab, N. Plastira 100, Vassilika Vouton, Irakleio, GR70013, Greece*

Received 29 August 2020; revised 10 December 2020; accepted for publication 17 December 2020

We still have little knowledge concerning the phylogeography of amphibians and reptiles from the Balkan Peninsula compared with the other two Mediterranean peninsulas. This raises concerns for endemic taxa from these peninsulas, because it might interfere with further conservation efforts. Here we focus on the endemic Greek stream frog (*Rana graeca*) and reconstruct its biogeography and evolutionary history. Using four genetic markers (*Cytb*, 16S, *COI* and *BDNF*) in > 350 sequences covering the whole distribution range, we conducted phylogenetic, demographic and ecological niche analyses, which revealed the phylogeography of this species. Surprisingly, this examination of *R. graeca* reveals a very shallow level of intraspecific genetic variability through the Balkans, with two main, statistically supported lineages having a partly sympatric distribution. The most variable marker was *Cytb*, which showed 19 haplotypes in 123 analysed sequences in the whole species distribution area. Here presented genetic data, together with the environmental niche projection and demographic analyses suggest that *R. graeca* was probably affected only marginally by climatic oscillations, with the Hellenides as the most suitable area for the occurrence of the species in different geological periods. This is consistent with the observed genetic diversity, which is mostly related to these mountains. Although the species shows a certain level of phenotypic variability and ecological preferences, this might be related to species plasticity affected by the micro-climatic conditions in small areas, which merits further research. Comparing phylogeography of other amphibian and reptile species in the Balkans, we showed that the observed pattern represents a new view on the phylogeography of the Balkan herpetofauna.

ADDITIONAL KEYWORDS: demography – Eastern Mediterranean – endemism – genetic diversity – phenotype – Pleistocene – *Rana graeca* – Ranidae.

INTRODUCTION

Biodiversity hotspots are areas with an exceptionally high ecosystem, species and genetic diversity (Hewitt, 2011). Examples of such regions in the Western Palaearctic are the Balkan Peninsula and/or overall Eastern Mediterranean. Their fauna has experienced dramatic shifts during past climatic and topographic changes, which has left a mark on their current species and genetic diversity (Schmitt & Varga, 2012; Salvi *et al.*, 2013; Poulakakis *et al.*, 2015; Jablonski *et al.*, 2016, 2019; Kindler *et al.*, 2018). The Balkans has a complex topography, with the presence of different mountain reliefs and numerous environmental niches that have preserved biodiversity during the Pliocene/Pleistocene climatic changes (Griffiths *et al.*, 2004). Compared with the other two southern European Peninsulas (Iberian and Italian), the Balkan Peninsula is phylogeographically less studied, although it is an important source of species diversity and endemism

*Corresponding author. E-mail: jablonski.dan@gmail.com

as a consequence of its role as the late Miocene radiation centre (Kryštufek *et al.*, 2007; Dufresnes *et al.*, 2013, 2019a, b; Poulakakis *et al.*, 2015). These endemics stayed located mainly in or around the Dinarides and Hellenides, which is why they mostly have small distribution ranges (Wielstra *et al.*, 2014, 2018; Jablonski *et al.*, 2016; Kotsakiozi *et al.*, 2018). A good example is the Peloponnese (south continental Greece), which hosts several endemic taxa either at the species level (e.g. *Anguis cephallonica*, *Algyroides moreoticus* and *Podarcis peloponnesiacus*) or at the genus level (*Hellenolacerta graeca*; Valakos *et al.*, 2008). Despite their small geographical ranges, some of these taxa are characterized by a higher level of intraspecific genetic diversity (Dufresnes *et al.*, 2013; Pabijan *et al.*, 2015; Psonis *et al.*, 2017, 2018; Spilani *et al.*, 2019).

Another endemic species in the Balkans is *Rana graeca* Boulenger, 1891 (Figs 1, 2), formerly considered also as a part of the Apennine frog fauna (*Rana graeca italica* Dubois, 1987). Picariello *et al.* (2002), however, showed that *R. italica* is not a subspecies of *R. graeca* but a different species. This was the opposite of the findings of Asimakopoulos (1994), who stated morphological uniformity between *R. graeca* and *R. italica*. Later, Veith *et al.* (2003) clearly confirmed the findings of Picariello *et al.* (2002) and showed that *R. graeca* forms a monophyletic clade with *Rana dalmatina* and *Rana latastei* and that this clade is sister to the clade of *Rana* species from the Anatolian and Caucasian region (Anatolian clade; Veith *et al.*, 2003). Both *R. graeca* and *R. italica* are currently recognized as endemic taxa. *Rana graeca* occurs in almost the whole of continental Greece, south-western Bulgaria, North Macedonia, Albania, southern and central Serbia and Montenegro and extends up to north-western Bosnia and Herzegovina, close to the Croatian border (Asimakopoulos & Grossenbacher, 2014; Sillero *et al.*, 2014; Šukalo *et al.*, 2015; Šunje *et al.*, 2017, 2018; Fig. 2). Interestingly, the species is missing in most of the large islands that are close to its mainland range (i.e. Corfu, Kefalonia, Lefkada and Zakynthos) except Thasos (North Aegean). This species often lives in valleys that have streams, springs or small rivers with cold, clear water. This species has a high vertical distribution, starting from sea level and reaching high mountain areas (≤ 2100 m a.s.l.; Stojanov *et al.*, 2011; Asimakopoulos & Grossenbacher, 2014; Szabolcs *et al.*, 2017). This might be an indication of the ecological plasticity of the species. This frog also shows a certain level of phenotypic variability (Bringsøe, 2011; Asimakopoulos

Figure 1. Individuals of *Rana graeca* from different geographical origins express different colour patterns. A, individual from the Theth valley, Albania. B, individual from Banjë, Albania. C, individual from Samarina, Greece. D, individual from Chora Getson, Peloponnese, Greece. Photographs by Daniel Jablonski.

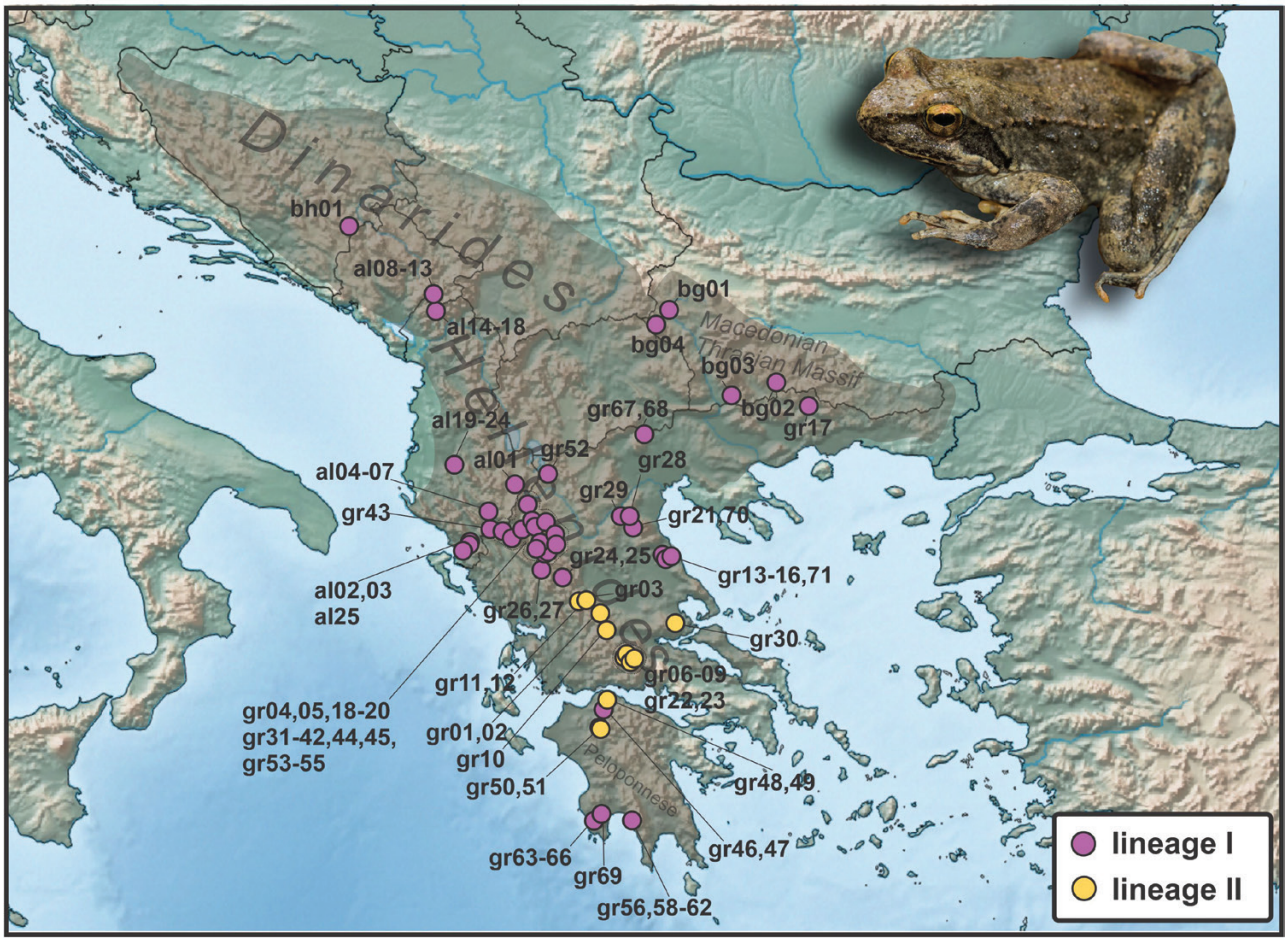

Figure 2. Geographical distribution of samples of the Greek stream frog (*Rana graeca*) used exclusively in our study, with colours corresponding to the main recovered phylogenetic lineages (for locality details of particular samples, see Supporting Information, Table S1). For geographical coverage including published sequences, see Figure 4. The distribution range of the species is indicated in dark brown (Asimakopoulos, 1994; Asimakopoulos & Grossenbacher, 2014; Sillero *et al.*, 2014; Šukalo *et al.*, 2015; Šunje *et al.*, 2017, 2018). The pictured specimen originates from the locality Lojmë, Albania.

& Grossenbacher, 2014; Fig. 1), which suggests that the external morphology could be interpreted as a genetic signal. We decided, therefore, to delve deeper into the evolutionary history of *R. graeca* based on molecular data, which are less known compared with other taxa of the genus (Veith *et al.*, 2003; Carranza & Arribas, 2008; Vences *et al.*, 2013; Canestrelli *et al.*, 2014; Yuan *et al.*, 2016; Teixeira *et al.*, 2018). The phylogeography of *R. graeca* was studied recently by Šunje *et al.* (2018), based on one mitochondrial DNA (mtDNA) marker and including only 22 samples along the distribution range of the species. The authors stated that a wider sampling and more genetic markers were required to resolve the evolutionary history of the species (Šunje *et al.*, 2018).

Herein, we investigate the multilocus intraspecific phylogeny and phylogeography of *R. graeca*, combining phylogenetic trees (gene trees and species trees), network and demographic analyses with past and current species distribution modelling. Our objectives were as follows: (1) to evaluate the evolutionary history, genetic diversity and phylogeography of the species; (2) to estimate demography and species range fluctuations; and (3) to carry out a biogeographical comparison of the studied species with amphibians and reptiles that are endemic in the continental Balkans.

MATERIAL AND METHODS

SAMPLE COLLECTION

In total, 101 *R. graeca* tissue samples were obtained from 55 localities of four countries and used in the phylogenetic, phylogeographical and demographic analyses, covering the whole species range (Fig. 2; Supporting Information, Table S1). The Natural

History Museum of Crete (NHMC) specimens ($N = 54$) have been collected during its research activities, for the most part the recording of the Greek Fauna through collections, from 1995 to the present, following the provisions of the Presidential Decree 67/81. Collected specimens, after a small abdominal dissection to allow ethanol to enter the body cavities, were stored initially in 96% ethanol, which was changed to fresh 96% ethanol upon return of the expedition members to the NHMC premises. For the present study, a small piece of muscle tissue from the thigh of the adult or, alternatively, from the tail of the tadpole was used. Other material was obtained from road-killed individuals (liver and muscle) or, alternatively, from living animals as blood droplets or a ting piece of a digit on the right hindleg.

To place our data into a phylogeographical context, we compiled an additional dataset supplemented by all known published sequences of *R. graeca* from the GenBank database (Veith *et al.*, 2003; Ilić *et al.*, 2016; Yuan *et al.*, 2016; Šunje *et al.*, 2018). These published sequences represent mostly the cytochrome *b* marker and come from Albania, Bosnia and Herzegovina, Greece, Montenegro and Serbia (Figs 2, 3; Supporting Information, Table S1).

Moreover, 13 *R. dalmatina* and two *Rana temporaria* from the southern Balkans (the NHMC collection) were also obtained and used in the phylogenetic and phylogeographical analyses. Additionally, six *R. dalmatina*, 15 *R. temporaria*, one *Rana pyrenaica*, one *Rana arvalis*, one *Rana asiatica* and one *Rana macrocnemis* were were retrieved from GenBank based on the availability of the genetic markers used in our study and used in phylogenetic analyses. Finally, 16 *Pelophylax* specimens (two *Pelophylax cretensis*, two *Pelophylax kurtmuelleri*, three *Pelophylax cerigensis* and nine *Pelophylax* cf. *bedriagae*) were also collected by the NHMC and used in the chronophylogenetic analyses (Supporting Information, Table S1), in which these specimens were used as external calibration points based on the results of previously published studies (Lymberakis *et al.*, 2007; Poulakakis *et al.*, 2013).

WET LAB AND SEQUENCING

Total genomic DNA from all sampled individuals was extracted using a standard ammonium acetate protocol (Bruford *et al.*, 1998) from muscle, liver or blood. Double-stranded polymerase chain reaction (PCR) was used to amplify partial sequences of three mitochondrial genes (mtDNA) encoding cytochrome oxidase subunit I (*COI*) and cytochrome *b* (*Cytb*) and the large ribosomal subunit (16S rRNA), in addition to one nuclear gene (nuDNA) encoding brain-derived neurotrophic factor (*BDNF*). Primers and conditions used in PCR amplification and in cycle sequencing reactions are given in the Supporting Information (Table S2). Single-stranded sequencing of the PCR product was performed using the Big-Dye Terminator (v.3.1) Cycle Sequencing kit on an ABI3730 automated sequencer, following the manufacturer's protocol and using the same primers as in the PCR. Sequences were viewed and edited using CODONCODE ALIGNER v.3.7.1 (CodonCode Corporation). The authenticity of the sequences and the homology to the targeted genes were evaluated with a BLAST search in the NCBI genetic database (http://blast.ncbi.nlm.nih.gov/Blast.cgi). All coding gene sequences (*Cytb*, *COI* and *BDNF*) were translated (DNASP v.6.0; Rozas *et al.* 2017) before further analysis, in order to check for the existence of stop codons.

All newly determined sequences have been deposited in GenBank (Supporting Information, Table S1). The alignment of the sequences was performed separately for each locus using the algorithm CLUSTALW as is implemented in MEGA X (Kumar *et al.*, 2018).

PHYLOGENETIC AND PHYLOGEOGRAPHICAL ANALYSES

In order to investigate the phylogenetic relationships, genetic diversity and demography of *R. graeca*, four datasets were constructed: (1) a concatenated DNA dataset with all four loci (16S, *Cytb*, *COI* and *BDNF*); (2) a concatenated DNA dataset with mitochondrial loci (16S, *Cytb* and *COI*); (3) a concatenated DNA dataset with 16S and *Cytb*, excluding *COI*, in order to access the effect of missing data (see Results section); and (4) a dataset with the nuclear marker (*BDNF*), all including *R. graeca*, *R. dalmatina*, *R. temporaria*, *R. pyrenaica*, *R. arvalis*, *Rana macrocnemis*, *R. asiatica* and *Pelophylax* spp. that were used as an outgroup.

The mtDNA alignment was partitioned into seven blocks, including three blocks for the first, second and third codon positions for the protein-coding locus *Cytb*, three blocks for the first, second and third codon positions for the protein-coding locus *COI*, and one block for 16S rRNA. Likewise, the nuDNA alignment (*BDNF*) was also partitioned into three blocks for its first, second and third codon positions (Supporting Information, Table S3). These initial partition schemes were loaded into PARTITIONFINDER v.2.1 (Guindon *et al.*, 2010; Lanfear *et al.*, 2017) in order to calculate and select the best-fitting partitioning scheme and evolutionary models. The results were implemented in each program (MRBAYES and RAXML), based on the Bayesian information criterion (BIC), the greedy algorithm and considering that the blocks of each alignment had linked branch lengths. The models that included both gamma distribution and invariable sites were ignored (Yang, 2006).

Phylogenetic reconstruction was conducted using two different approaches, maximum likelihood (ML)

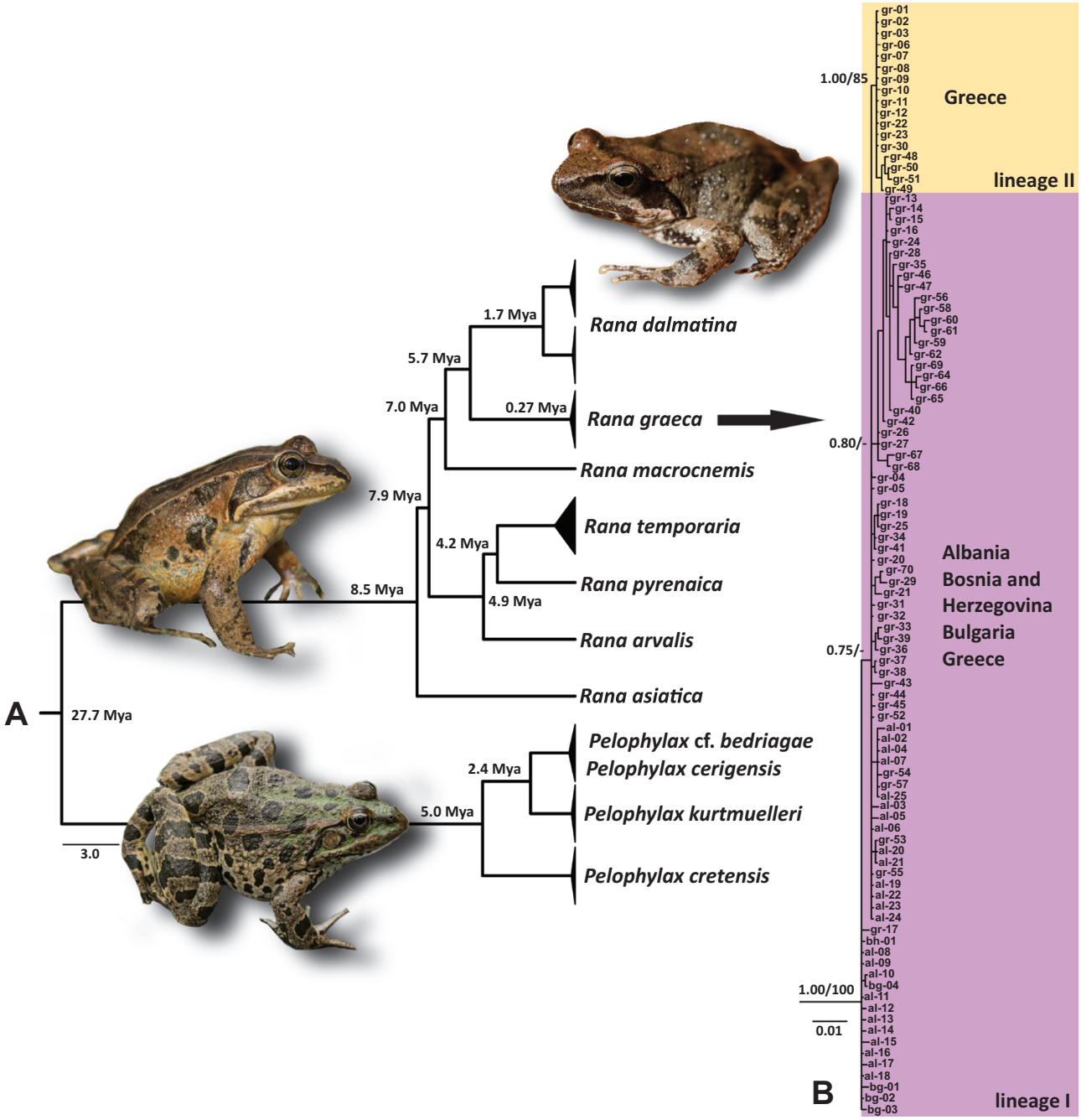

Figure 3. A, the dated phylogeny of the genus *Rana*, showing the studied species. Numbers between clades of species show the estimated time of divergence (in millions of years ago). B, the Bayesian tree reconstructed from the concatenated dataset (2707 bp; Supporting Information, Table S1), rooted with the sequence of congeneric sister species (*Rana dalmatina* and *Rana temporaria*) and *Pelophylax* spp. (not shown). Numbers above the branches show posterior probabilities/maximum likelihood bootstrap support values. The scale bar corresponds to one substitution per 100 nucleotide positions. Each terminal branch represents a sample with its locality number (see also Fig. 2; Supporting Information, Table S1). Phylogenetic lineage colours correspond to those used in Figures 2 and 4.

and Bayesian inference (BI). The same parameters were used for all datasets. Maximum likelihood analyses were performed using RAxML v.8.1.21 as implemented through RAXMLGUI v.1.5 (Silvestro & Michalak, 2011). The best ML tree for each dataset was selected from 50 iterations, and the confidence

of the branches was assessed further based on 1000 thorough bootstrap replicates. Bayesian inference analyses were conducted in MRBAYES v.3.2.7 (Ronquist *et al.*, 2012), with four runs and eight Markov chain Monte Carlo (MCMC) chains per run for 2×10^7 generations, sampling every 1000th generation. Several MCMC convergence diagnostics were used to check for convergence and stationarity [the plot of the generation vs. the log probability of the data (the log-likelihood values), the average standard deviation of split frequencies, the average potential scale reduction factor, and the minimum value of minimum estimated sample sizes (ESS)]. The lnL was stabilized after ~6×10^6 generations for the mitochondrial and the combined analysis and after 2×10^6 generations for the analysis of the nuclear dataset. The first 35% (7×10^6) trees were discarded as burn-in, as a measure to sample from the stationary distribution and avoid the possibility of including random, suboptimal trees. A majority-rule consensus tree was then produced from the posterior distribution of trees, and the posterior probabilities were calculated as the percentage of samples recovering any particular clade. Posterior probabilities ≥ 0.95 indicate statistically significant support (Huelsenbeck & Ronquist, 2001).

Given that a network approach can sometimes generate a more effective presentation of the intraspecific evolution than the tree-based phylogenetic approaches (Posada & Crandall, 2001), we also constructed haplotype networks for three mtDNA and one nuclear gene using the 95% limit of parsimony (TCS algorithm) as implemented in the software POPART (http://popart.otago.ac.nz). The resultant phylogenetic pattern was then presented according to the frequency of a particular lineage in the haplotype network. For network analyses, we compared overall 382 sequences (107 sequences from 16S of 387 bp, 123 from *Cytb* of 322 bp, 53 from *COI* of 631 bp, and 99 from *BDNF* of 453 bp; Supporting Information, Table S1) with the same sequence length for the particular marker.

DIVERGENCE TIME ESTIMATIONS

The species tree and divergence times of *Rana* species in the southern Balkans were estimated using the dataset containing both mtDNA and nuDNA sequences using the Standard Template BEAST 2 package as implemented in BEAST 2 v.2.6.2 (Bouckaert *et al.*, 2019). The input files (xml format) were created using BEAUTI v.2.6.2. We used two unlink partitions, one for mtDNA (unlinked site and clock models and linked trees) and one for nuDNA. We used the model averaging tool BMODELTEST (Bouckaert & Drummond, 2017) to select the most appropriate substitution model. The Yule model for speciation and the uncorrelated lognormal model for describing the molecular clock were selected. Regarding the divergence time estimation, a calibration point retrieved from the study on *Pelophylax* phylogeny was used (Lymberakis *et al.*, 2007): the split of *P. cretensis* from all other *Pelophylax* species at ~5–5.5 Mya, using normal distribution. This calibration point is based on a very well-known paleogeological event, which is the permanent isolation of the island of Crete from the Peloponnese (Meulenkamp, 1985; Dermitzakis, 1990). For this reason, we included in the analysis the corresponding sequences of *P. cretensis*, *P. kurtmuelleri*, *P.* cf. *bedriagae* and *P. cerigensis*. The MCMC analysis was run for 6×10^8 generations, saving the result every 5×10^3 generations. The first 25% of the saved trees were discarded after inspection of the log files with TRACER v.1.6 (Rambaut *et al.*, 2014). The maximum clade credibility (MCC) tree that best represented the posterior distribution was identified using TREEANNOTATOR v.2.6.2 (also included in BEAST 2).

DNA POLYMORPHISM AND DEMOGRAPHY

The sequence divergence (*p*-distances) was estimated using MEGA X. The program DNASP v.6.0 (Rozas *et al.*, 2017) was used to estimate the number of haplotypes (h), haplotype diversity (h_d), number of segregating sites (S), nucleotide diversity (π) and Watterson's theta per site (θW).

The past population dynamics were inferred using the Bayesian coalescent-based approach of the Bayesian skyline plot (BSP; Drummond *et al.*, 2005), as implemented in BEAST 2. This method computes the effective population size through time directly from sampled sequences and does not require a specific a priori assumed demographic model. This method was applied for all *R. graeca* sequences of the *Cytb* dataset owing to the highest number of available sequences of this variable marker. We used the methodology of Vences *et al.* (2013), a uniform prior for the mean substitution rate with the initial value of 0.005 mutations per site/Myr. Preliminary analyses were run using both a strict molecular clock and the uncorrelated lognormal relaxed molecular clock. Given that the parameter of the standard deviation of the uncorrelated lognormal relaxed clock was close to zero, the final analyses were run enforcing the strict molecular clock model. Using PARTITIONFINDER, all codon positions being treated together as one partition was selected as the best-fitting partitioning scheme, and the HKY substitution model was selected as the best-fitting model. The final BSP analysis was run in duplicates to check for consistency between runs, each run for 10 million generations and sampled every 1000 generations. Convergence, ESS > 200, stationarity and the appropriate number of generations to be discarded as burn-in (10%) were assessed using TRACER. The

resulting BSP was also summarized in TRACER, with the maximum time as the median of the root height parameter. In addition, the mismatch distributions (MD) were calculated as the distributions of the observed pairwise nucleotide differences and the expected values under a growing- or declining-population model using DNASP. The occurrence of historical demographic changes was assessed with neutrality-test statistics (Fu's F_S and Tajima's D) implemented and calculated in DNASP, with the estimation of the statistical significance using 10 000 coalescent simulations. Negative significant values of F_S and D are expected when population expansion occurs (Tajima, 1989; Fu, 1997).

SPECIES DISTRIBUTION MODELLING

The occurrence dataset of the Greek frog (*R. graeca*) was constituted by 1067 points from field campaigns, citizen science databases (GBIF, 2020; Ueda, 2020), the literature or our own databases (Supporting Information, Table S4). The area of the modelling was based on the current species distribution (Šunje *et al.*, 2018) along with implications for possible past range in the context of the Balkan Peninsula. The environmental data are based on bioclimatic variables from the CHELSA database (Karger *et al.*, 2017) for the current climate and from the PaleoCLIM database for the past conditions, the Last Glacial Maximum (LGM) and the Mid-Holocene (Fordham *et al.*, 2017; Brown *et al.*, 2018), at 5 km pixel size. The spThin R package (Aiello-Lammens *et al.*, 2015) and an occurrence thinner radius of 5 km were used for the minimization of any effect of sampling bias (Boria *et al.*, 2014). The use of the USDM R package (Naimi *et al.*, 2014) has been selected for calculation of the variance inflation factor (VIF) for the set of selected predictors and excludes the highly correlated variables from the set through a stepwise procedure (VIF values < 10; Dormann *et al.*, 2013). The WALLACE R package (Kass *et al.*, 2018) was used for the modelling, allowing the fine-tuning (Hao *et al.*, 2020) of the MAXENT algorithm using the ENMEVAL R package (Muscarella *et al.*, 2014). The 'block' geographical partition scheme of ENMEVAL was selected for all the analyses (Muscarella *et al.*, 2014) because it split the dataset into four different independent datasets across longitudinal and latitudinal directions (Supporting Information, Table S5; Fig. S1) for training/validation. ENMEVAL allowed us to evaluate models using a geographical partitioning scheme and to 'fine-tune' two parameters of MAXENT that affect model complexity and predictive power. These parameters are the regularization multiplier (RM) or beta values and the feature classes (FCs). The RM penalizes overly complex models, whereas the FCs are functions of the raw environmental data (Morales *et al.*, 2017). All FCs (L = linear, Q = quadratic, H = hinge and P = product) were selected, and the RM was set between one and five with steps of 0.5, allowing for model complexity and model tuning. Basically, all predictor variable coefficients were shrunk progressively until some reached zero, when they dropped out of the model. Only those variables with the greatest predictive contribution remained in the mode (Supporting Information, Table S6). The model selection was based on the average test Area Under Curve value (avg.test.AUC) along with the lowest delta corrected Akaike information criterion (delta.AICc) as calculated for each model following the method of Warren & Seifert (2011). In total, 45 different models were built, run and tested. A threshold rule distinguishing area with 'suitable' vs. 'unsuitable' climatic conditions was applied; we adopted the commonly used 'minimum training presence threshold' (Radosavljević & Anderson, 2014), and a 'stability' map was also created by assembling all of the model projections, that is, depicting as 'suitable' only the pixels that were predicted as 'suitable' by all of the model projections. The final maps were designed in ARCGIS v.10.5 (Environmental Systems Research Institute, 2019).

COMPARISON WITH ENDEMIC SPECIES OF AMPHIBIANS AND REPTILES IN THE BALKANS

To compare the genetic diversity of *R. graeca* with other endemic species of amphibians and reptiles distributed in the continental Balkans (*sensu* Speybroeck *et al.*, 2016), we compared available mitochondrial protein-coding gene sequences that have a similar substitution rate (Johnson & Sorenson, 1998): *Cytb* and NADH dehydrogenase subunits II–IV (*ND2*, *ND3* and *ND4*; overall, 631 sequences) for seven amphibians and 17 reptiles (however, data for two *Algyroides* species and *Podarcis erhardii* were unavailable; for details see Supporting Information, Tables S7 and S8). For 21 species, we calculated the nucleotide diversity (π), haplotype diversity (h_d) and number of haplotypes using DNASP. The threshold for describing genetic diversity was considered as follows (π): 0–1%, low level; 1–2.5%, medium; and > 2.5%, high. This diversity was also put into the context of approximate species ranges *sensu* Sillero *et al.* (2014), Speybroeck *et al.* (2016). The area of the distribution range was estimated using QGIS (QGIS Development Team, 2020). Moreover, we gathered the expected time of divergence for these endemic species based on available published data (Supporting information, Table S8). We performed general linear model (GLM) analysis to investigate possible relationships between the size of the species distribution range and the genetic diversity and between the age of divergence

and the genetic diversity. We tested both the haplotype (h_d) and the nucleotide diversity π (expressed as a percentage). We used the ***GeoDa*** python application (Anselin *et al.*, 2006) for normal ordinary least squares (OLS) and R (R Core Team, 2020) for GLM with Poisson family using the built-in GLM of core R, and we used the rsq R package (Zhang, 2020) for the calculation of R^2 values for each combination.

RESULTS

PHYLOGENY AND PHYLOGEOGRAPHY

We obtained a total of 351 sequences (99 sequences from 16S, 101 from *Cytb*, 53 from *COI* and 98 from *BDNF*) of *R. graeca* and 121 outgroup sequences (*Rana* spp. and *Pelophylax* spp.), with no signal of contamination or sequences of nuclear genomic origin (Supporting Information, Table S1). Analyses of saturation tests for each gene separately did not show any evidence of saturation (data not shown). Together with outgroup sequences, a total alignment length of 2707 bp was analysed. The best-fitting partitioning schemes for each downstream analysis and the selected nucleotide substitution models are presented in the Supporting Information (Table S3). Both datasets (mtDNA and mtDNA + nuDNA) identified only two lineages with similar tree topologies after ML (lnL = –7985.72) and BI analysis (lnL = –8073.12; Figs 2, 3B). For the mtDNA datasets (with and without *COI*), the ML and BI showed similar topologies (see Supporting Information, Figs S2–S7), which were in accordance with the topologies of the complete dataset with lnL = –6727.10 and –6851.08 (mtDNA dataset) with all mitochondrial gene fragments and lnL = –4214.19 and –4345.71 (mtDNA dataset) with all mitochondrial gene fragments except *COI*, respectively. Unfortunately, for the *BDNF* marker, sequences were not available in GenBank for the species *R. pyrenaica*, *R. arvalis*, *R. macrocnemis* and *R. asiatica*, and the analyses were restricted to *R. graeca*, *R. dalmatina* and *R. temporaria*. For *BDNF*, ML and BI produced similar topologies, in which *R. graeca* appeared monophyletic (lnL = –1062.54 and –1111.07 for ML and BI, respectively), as for the mtDNA trees, but without any intraspecific differentiation.

All MCMC diagnostic metrics indicated that the iterations of BI analysis reached convergence and stationarity. The average standard deviation of split frequencies was 0.009 for the complete dataset and 0.007 for the mtDNA dataset (when this value approaches zero, the tree samples are more similar), and the plot of generation vs. log-likelihood of the data had a characteristic 'white-noise' morphology after burn-in. In addition, for all parameters, the potential scale reduction factor values were 1.000 in both datasets, and the minimum ESS values were > 200 for all parameters in both datasets. According to the chronophylogenetic analyses of the concatenated dataset (lnL = –6917.64, ESS > 1070), the temporal time of divergence of the European *Rana* was estimated as 7.9 Mya (Tortonion age in the Late Miocene), with the divergence of the *R. temporaria* group from its sister clade that includes *R. graeca*, *R. macrocnemis* and *R. dalmatina*. The divergence of *R. graeca* and *R. dalmatina* was estimated to have occurred during the Messinian Salinity Crisis (MSC) in the Messinian age (Late Miocene; 5.7 Mya), whereas the intraspecific differentiation of *R. graeca* was dated to the Late Pleistocene (0.27 Mya) (Fig. 3A).

The resulting topology of *R. graeca* represented an unexpected and very shallow divergence, with two main statistically supported lineages (I and II). The highest recorded *p*-distance between lineages of the concatenated dataset was 0.67%, and overall nucleotide diversity was only 0.46%. Lineage I had a nucleotide diversity of 0.410% (N = 82) and lineage II 0.077% (N = 17). Lineage I included specimens collected in the Dinarides (northern Albania, Bosnia and Herzegovina), Hellenides (southern Albania and northern Greece), the Macedonian–Thracian Massif (Rhodopes; eastern Bulgaria and north-eastern Greece) and Peloponnese. Lineage II was distributed in the central and southern Hellenides and northern Peloponnese. Lineages I and II were recorded in sympatry only in north Peloponnese (gr46–gr49; Fig. 2).

Haplotype networks showed a different level of differentiation depending on the DNA marker used (the highest level was in mitochondrial *Cytb* and the lowest in nuclear *BDNF*; Fig. 4). Both lineages were well recognized in *Cytb*, containing unique haplotypes that were separated from the central and most common haplotype by two mutation steps (Fig. 4). The geographically marginal populations from Bosnia and Herzegovina or Bulgaria were detected in the central haplotype of lineage I.

Seventeen haplotypes were recognized in 107 sequences of 16S, with h_d = 0.53 and π = 0.19% (Table 1). Both lineages were revealed, with only two haplotypes from southern mainland Greece and the northern Peloponnese belonging completely to lineage II (Fig. 4).

In 123 sequences of *Cytb* spaced across the Balkans, we found 19 haplotypes, with h_d = 0.87% and π = 0.78% (Table 1). Fifteen out of 19 haplotypes corresponded to lineage I, and lineage II contained four haplotypes from the central and southern Greece and the northern Peloponnese (Fig. 4).

Only nine haplotypes were revealed among the 53 sequences of *COI*, with h_d = 0.70 and π = 0.23% (Table 1). Only lineage I was distinct in the network (Fig. 4), and lineage II was observed sharing haplotypes with the lineage across the Greek part of the Hellenides (Fig. 4).

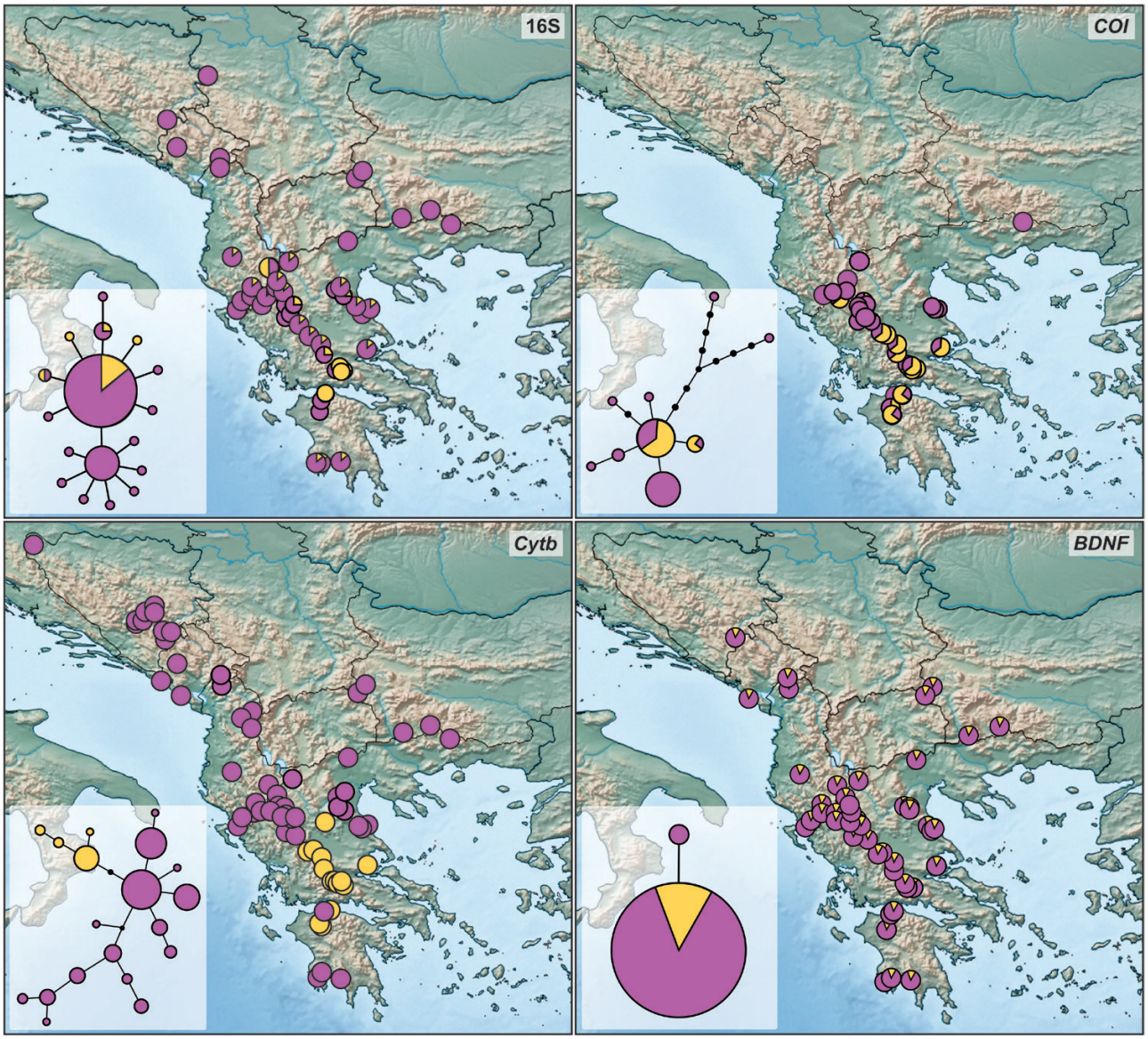

Figure 4. The phylogeographical pattern of *Rana graeca* based on particular markers and according to the lineage affiliation of the localities in light of the concatenated tree (Fig. 3). Phylogenetic lineage colours correspond to those used in Figures 2 and 3.

In the highly conservative nuclear marker (*BDNF*), only two haplotypes were revealed among the 99 sequences analysed, with very low h_d (0.04) and π (0.009%) (Table 1). One was present in both lineages, distributed from south-eastern Bosnia and Herzegovina to the southern Peloponnese. The only haplotype that corresponded completely with lineage I was found in one locality in north-eastern Greece (Fig. 4).

DEMOGRAPHY

The Bayesian skyline plot analysis on *Cytb* (Fig. 5A) showed a slight population growth (N_e) of *R. graeca*, which started at ~15 kya, close to the end of the last glacial period. The observed value of complementary mismatch distributions (MDs; Fig. 5B) mirrored the expected value for a growing- or declining-population model. The neutrality tests showed no significant evidence of an expansion (F_S = −0.18520, P = 0.549; Tajima's D = −0.067, P = 0.445).

SPECIES DISTRIBUTION MODELLING

From the initial 1067 occurrence data points (656 unique locations), 337 occurrence data points were included in the final model (Supporting Information, Tables S4 and

Table 1. Summary of DNA polymorphism for concatenated dataset of *Rana graeca* and particular genes

	Length (bp)	*N*	*h*	*S*	π ± SD (%)	h_d ± SD	θ*W* ± SD (%)
Rana graeca	2707	99	33	27	0.46 ± 0.027	0.93 ± .0.011	0.74 ± 0.23
16S	387	107	17	15	0.19 ± 0.025	0.53 ± 0.055	0.75 ± 0.26
Cytb	322	123	19	15	0.78 ± 0.054	0.87 ± 0.017	0.87 ± 0.30
COI	631	53	9	18	0.23 ± 0.059	0.70 ± 0.045	0.64 ± 0.23
BDNF	453	99	2	1	0.009 ± 0.006	0.04 ± 0.027	0.04 ± 0.04

Abbreviations: *h*, number of haplotypes; h_d, haplotype diversity; *N*, number of species; π, nucleotide diversity; *S*, number of segregating sites; SD, standard deviation; θ*W*, Watterson's theta per site.

S5). From the predictors after the VIF analysis, we ended up with eight out of 19 initial predictors; these were the isothermality (bio_3), temperature seasonality (bio_4), maximum temperature of the warmest month (bio_5), mean temperature of the wettest quarter (bio_8), mean temperature of the driest quarter (bio_9), precipitation seasonality (bio_15), precipitation of the warmest quarter (bio_18) and precipitation of the coldest quarter (bio_19) (Supporting Information, Table S6). Forty-five models were run consecutively, and the model with the lowest delta.AICc was the one that used hinge (H) features along with a regularization multiplier of two (H_2). The AUC was high for both train.AUC (0.9) and avg.test.AUC (0.84); it is worth mentioning that almost all models had high AUC values (> 0.85). The projections in the present, LGM and Mid-Holocene climate periods showed a stabile overall spatial coverage (where the species might occur), but with a vast reduction of its distribution in the Mid-Holocene (with appearance in some new areas, i.e. east Greece and European Turkey) and a slow spread in the current period (Fig. 6). The congruence of models showed that the species distribution was confined to the territory of the Balkan Peninsula, with some new potential areas of occurrence, i.e. where the presence of the species has not yet been confirmed (the Dinarides in Croatia, the Balkanides in Bulgaria or European Turkey). The most stable conditions across all models were detected in the south-western Balkans and the Peloponnese, corresponding to the Hellenides. The most important variables were bio_3, bio_44, bio_18 and bio_19, related to temperature and to rainfall (Fig. 6; Supporting Information, Table S6).

Rana graeca and other endemics

Our comparative dataset of 24 endemic species of amphibians and reptiles from the continental Balkan Peninsula showed that *R. graeca* had the second-lowest value of genetic/nucleotide diversity (19 haplotypes with π = 0.78%) among the endemic amphibians and sixth lowest of all species (Supporting Information, Table S8), with the expected time of divergence dated at 5.7 Mya. In contrast, *R. graeca* was the species with the largest distribution range among the examined endemic taxa (~220 000 km²). The available published data of expected times of divergence showed that speciation of inspected endemic taxa of the Balkans occurred between ~16 and 3 Mya (the Miocene to Pliocene). For three species, we are missing comparative molecular data. Finally, 15 of those endemic species are biogeographically associated mostly with the Hellenides, but only six with the Dinarides and three (including the focus species) with both of them (Supporting Information, Table S8). No statistical evidence has emerged using OLS or GLM with Poisson family ($R^2 < 0.005$), and it cannot support any relationships between the examined variables.

DISCUSSION

EVOLUTIONARY HISTORY

Five species of the genus *Rana* (*R. arvalis*, *R. dalmatina*, *R. graeca*, *R. latastei* and *R. temporaria*), from two different evolutionary groups (Veith *et al.*, 2003; Yuan *et al.*, 2016), are found in the Balkan Peninsula (Ilić *et al.*, 2016; Speybroeck *et al.*, 2016). Our knowledge of their evolutionary history is, however, limited in comparison to that of other amphibians in the region (e.g. *Ichthyosaura*, *Triturus*, *Bombina*, *Bufotes*, *Pelobates* and *Pelophylax*; Lymberakis *et al.*, 2007; Fijarczyk *et al.*, 2011; Wielstra *et al.*, 2012, 2013; Recuero *et al.*, 2014; Vucić *et al.*, 2018; Dufresnes *et al.*, 2013, 2019a, b). The reason is that there was less sampling effort in previous studies, which did not allow the resolution of relationships among the Balkans and other populations of *Rana* species from Europe (Babik *et al.*, 2004; Vences *et al.*, 2013; Canestrelli *et al.*, 2014; Dufresnes *et al.*, 2020). Therefore, this needs further attention. As our data suggest, genetic variability among members of the genus in the Balkans is expected to be higher than is currently known (see *R. dalmatina* and

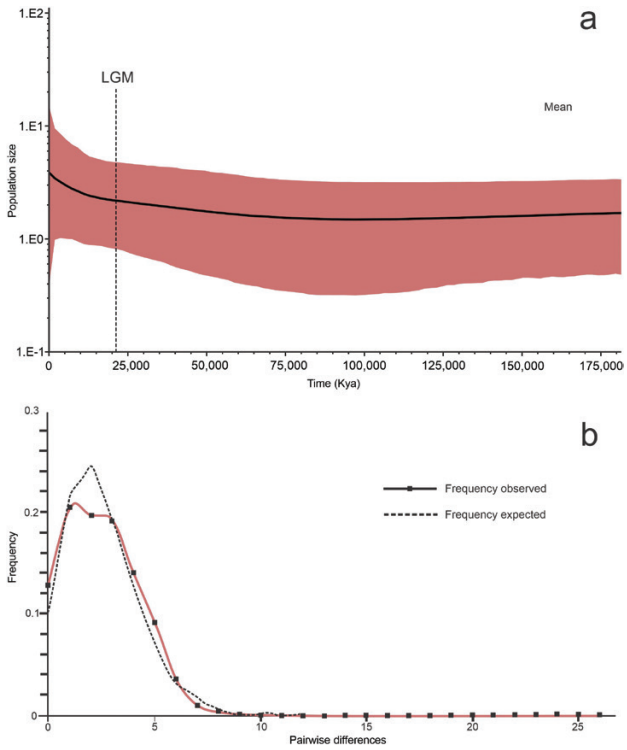

Figure 5. A, historical demography of *Rana graeca* estimated with Bayesian skyline plots. The central line shows the mean value of the population size [$N_e \times \tau \times \mu$; where N_e is the effective population size, τ is the generation length in units of time (substitutions/site), and μ is the mutation rate] on the logarithmic scale, and the shaded area represents the 95% highest posterior density. LGM indicates the time of the Last Glacial Maximum. B, mismatch distributions of observed frequencies (dashed line) compared with the expected frequencies (continuous line) under the expansion model of population size.

R. temporaria; Fig. 3; Supporting Information, Figs S2–S7).

In our phylogenetic analyses, *R. graeca* is a monophyletic species showing close relationships to *R. dalmatina* and *R. macrocnemis*. This is consistent with previously published studies, in which *R. graeca*, *R. dalmatina*, *R. macrocnemis* and *R. latastei* form a monophyletic clade (Picariello *et al.*, 2002; Veith *et al.*, 2003; Yuan *et al.*, 2016; Dufresnes *et al.*, 2020). This clade has a sister relationship with the *R. temporaria* species group that includes *R. arvalis*, *R. pyrenaica*, *R. parvipalmata*, *R. iberica* and *R. italica*. From the chronophylogenetic point of view, our estimated time of divergence supported the split of the European *Rana* in the Late Miocene (7.9 Mya; Fig. 3A). This is relatively close to the estimated radiation presented by Veith *et al.* (2003), but much younger than estimations by Yuan *et al.* (2016). According to Yuan *et al.* (2016), the European *Rana* diverged in the early Miocene (19 Mya), whereas the time differentiation of *R. graeca* from its sister lineages (*R. dalmatina*) was in the middle Miocene (12 Mya). This major discrepancy is probably attributable to the different calibration strategy (species tree approach vs. gene tree approach) used in our study compared with the study of Yuan *et al.* (2016). Moreover, our calibration was based on previous age estimations vs. the combination of fossils and age estimations used by Yuan *et al.* (2016). However, our estimations seem more reliable because they are closer to the MSC, confirming the current hypothesis about numerous speciation events during the late Miocene period (e.g. Dufresnes *et al.*, 2018, 2019a, b). Thus, *R. graeca* represents an old lineage, probably with a Miocene common ancestor, that became the endemic brown frog of the Balkan Peninsula, similar to the way in which *R. italica*, *R. iberica*, *R. parvipalmata*, *R. pyrenaica* or *R. tavasensis* became endemics for Apennine, Iberian or Anatolian Peninsulas (Veith *et al.*, 2003; Yuan *et al.*, 2016; Dufresnes *et al.*, 2020).

PHYLOGEOGRAPHY

Rana graeca showed a low level of intraspecific genetic diversity in view of its large range size (the largest among other endemic amphibians and reptiles of the Balkans), as shown by the concatenated markers and by the single markers (Figs 3, 4). In general, the two genetically shallow lineages revealed in

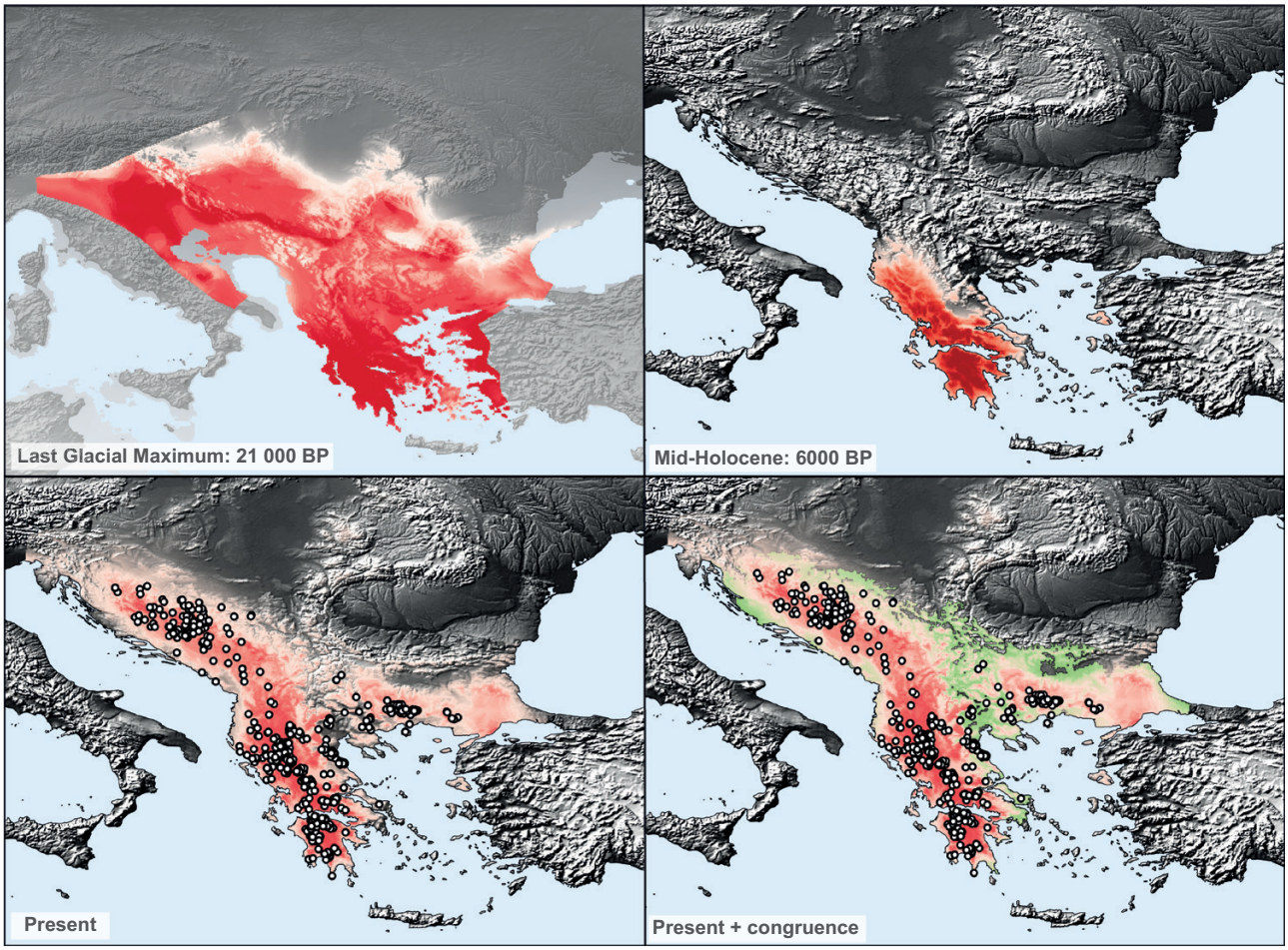

Figure 6. The environmental niche model projection on climatic conditions at the Last Glacial Maximum (LGM), Mid-Holocene, the present and a congruence of all models (green colour) for *Rana graeca* among geological times. White circles represent georeferenced occurrence records obtained from our own field research, publications and citizen science databases. The maps were designed in ARCGIS v.10.5 using Min-Max as the stretching histogram and bilinear interpolation as smoothing for display needs only.

R. graeca showed a certain phylogeographical pattern, whereby lineage I was distributed in the major part of the species range, whereas lineage II was limited to central and southern parts (Greece). Concurrently, these lineages formed a partly sympatric distribution pattern (Figs 2, 4).

In the richest dataset of 123 sequences of *Cytb* throughout the Balkans, we found 19 haplotypes distributed from the southern Peloponnese to north-western Bosnia and Herzegovina and western Bulgaria, also with very low intraspecific genetic variation. This variation was even lower in the case of the remaining analysed datasets (16S, *COI* and *BDNF*; Fig. 4). In the *Cytb* network analysis, two lineages of the concatenated dataset were recognized, separated by two mutation steps and partly suggesting a star-like pattern. Despite extensive sampling, our data did not show any significant hotspot of deeper genetic diversity suggestive of geographically limited microrefugia, as was presented for other species of the genus in Europe (Canestrelli *et al.*, 2008, 2014; Vences *et al.*, 2013; Teixeira *et al.*, 2018; Dufresnes *et al.*, 2020). The observed genetic pattern was, in contrast, very similar to that of *R. pyrenaica* (representative of the mountain Pyrenean endemism), suggesting very rapid colonization of its present small range (Carranza & Arribas, 2008). Likewise, the lineages of *R. graeca* probably diverged in a very narrow spatial and temporal window with subsequent rapid colonization, and possible extinction of peripheral populations, resulting in the observed low divergence between detected lineages and haplotypes (p-distances $\leq 0.62\%$). This corresponds to the so-called 'R' species model (Recuero & García-París, 2011) characterized by reduced genetic diversity, which was also observed in some other European brown frogs (Canestrelli

et al., 2008; Vences *et al.*, 2013; Teixeira *et al.*, 2018). Although low genetic diversity accompanied by a star-like phylogeographical structure often predict past population growth (Slatkin & Excoffier, 2012), this was not significantly supported here by neutrality tests (Fu's F_S and Tajima's D). Therefore, we can hypothesize that the Hellenides, as such, were probably the major centre for the species divergence and further evolution and colonization (Figs 2–4, 6), supporting the biogeographical importance of these south European mountains (Poulakakis *et al.*, 2015; Jablonski *et al.*, 2016; Marzahn *et al.*, 2016; Psonis *et al.*, 2017, 2018).

Šunje *et al.* (2018) suggested that dispersal of *R. graeca* in the Pleistocene was probably ongoing during warm phases and was restricted by climatic oscillations and geographical barriers, e.g. mountain glaciers. Surprisingly, however, our data suggested the opposite results and are in concordance with the presumption of Teixeira *et al.* (2018) that Mediterranean populations of *Rana* are currently surviving in interglacial refugia. This is unexpected, because the Plio-Pleistocene climatic changes are considered to be factors behind the diversified phylogeographical patterns observed today (Fijarczyk *et al.*, 2011; Pabijan *et al.*, 2015; Jablonski *et al.*, 2016; Dufresnes *et al.*, 2019b). First, based on genetic data (*Cytb*), the colonization of northern, eastern and southern areas, outside of the Hellenides, was probably conducted by several haplotypes very close to those from the central range (Fig. 5). More precisely, northern populations (Bosnia and Herzegovina, Montenegro and Serbia) were formed by three haplotypes that are close to those occurring in Albania or Greece (Fig. 4). Second, the SDM projection showed a possible range expansion of the species during the LGM and contraction during the warmest middle Holocene, probably followed by another expansion that was subsequently observed in the present model and corresponds to the known species range (Figs 2, 6).

This is also supported by demographic analysis, showing slight growths in population from around the LGM until today, but no significant population expansion. Similar results have been observed in several taxa (e.g. Stewart *et al.*, 2010), for which climatic conditions during the LGM were probably more suitable for population growth and/or range expansion compared with the warmer periods. Such a pattern was observed in very few cases of western Palaearctic amphibians (mainly cold-adapted species; Teixeira *et al.*, 2018; Afroosheh *et al.*, 2019). These species occur in lower-elevation areas during the LGM and then shift to higher altitudes. However, this cannot be fully applicable for *R. graeca*, because this frog is currently known from sea level or even thermal springs (Bringsøe, 2011; Šunje *et al.*, 2017; D. Jablonski, personal observations) up to high mountains (e.g. Szabolcs *et al.*, 2017). The observed long-term stability in the evolutionary history of *R. graeca* located in the south-western part of the peninsula therefore represents a new view of the phylogeography of the Balkan fauna with the following conclusions: (1) *R. graeca* is currently associated with regions of main mountain ranges of the Balkans, i.e. lineage I mostly in the Dinarides, Macedonian–Thracian Massif, northern and central Hellenides and lineage II in the southern Hellenides, including Peloponnese; (2) the species shows relative genetic homogeneity, with one geographically widespread lineage and a second, probably sympatric lineage inside the species range; and (3) the morphological and ecological differentiation observed in the species (Bringsøe, 2011; Asimakopoulos & Grossenbacher, 2014) is not mirrored in a phylogeographical signal of the markers studied. This means that *R. graeca* did not diversify in deeper phylogenetic lineages that could have a connection to certain historical microrefugia and/or be mirrored in the observed phenotypic variability. This suggests that the main influences were probably caused by microclimatic and local environmental conditions rather than past, long-term climatic cycles. Concurrently, the morphological variability (colour and pattern variation) and environmental adaptability of the species (type of the habitat, wide elevational range) are probably attributable to the phenotypic and ecological plasticity of the species, a fact which calls for further research (see also Šunje *et al.*, 2017).

Endemism in the Hellenides

Rana graeca is one of 24 endemic species of amphibians and reptiles in the continental Balkans (Supporting Information, Table S8). Although it has the largest distribution range among all endemic herpetofauna living there, its genetic diversity is very low. This could probably be attributed to the evolutionary history of the species (rapid colonization with a limited level of genetic variability), ecology or its overall natural history (the species mainly follows river valleys). Two phylogenetically supported lineages found in *R. graeca* have different sizes of the detected range, whereby the smaller (lineage II) is restricted to the southern Balkans and should be considered as a separate unit from the conservation point of view. As shown by our comparison (Supporting Information, Table S8), different levels of genetic diversity, range size or estimated time of divergence could be found among amphibians and reptiles endemic to the Balkans, especially in the Hellenides, e.g. cold-tolerant species showing a low

level of genetic diversity in small areas of distribution (*Vipera graeca*; Mizsei *et al.*, 2016, 2017) or species with larger distribution ranges influenced by long-term climatic oscillations that resulted in a high level of genetic diversity (e.g. *Anguis graeca*, *Mediodactylus kotschyi* and *Podarcis ionicus*; Jablonski *et al.*, 2016; Psonis *et al.*, 2017, 2018; Kotsakiozi *et al.*, 2018). We did not find relationship between the age of divergence and the level of currently observed genetic diversity or the size of the species range. However, this comparison is only general, and it needs further comprehensive research. Despite a wide current species distribution, the evolution of the specie´s is most probably associated mainly with the Hellenides. Despite the wide current distribution of *R. graeca*, the evolution of this frog has been most probably connected with the Hellenides. The Hellenides, partly shared with the Dinarides, represent 63% (15 species) of the overall continental Balkan herpeto-endemism (Supporting Information, Table S8) and are one of the most important biodiversity hotspots in the Eastern Mediterranean. This is definitely a topic for further evolutionary research and conservation priorities, in addition to the presented view of these southern European mountains as sources of species, genetic, or ecological diversity.

ACKNOWLEDGEMENTS

We would like to thank P. Balej, V. Gvoždík, D. Jandzik, M. Meszáros, P. Mikulíček, E. Mizsei, S. Papežíková, J. Poláková, M. Raffaj, E. Themeli and B. Vági for donation of samples, technical support or help in the field. We are also grateful to M. K. Lawson, S. R. Goldberg (who helped us with English) and Emina Šunje, in addition to three anonymous reviewers, for their comments, which significantly improved the first submitted version of the manuscript. This work was supported by the Slovak Research and Development Agency under the contract numbers APVV-15-0147 and APVV-19-0076.

REFERENCES

Afroosheh M, **Rödder D**, **Mikulíček P**, **Akmali V**, **Vaissi S**, **Fleck J**, **Schneider W**, **Sharifi M. 2019.** Mitochondrial DNA variation and Quaternary range dynamics in the endangered Yellow Spotted Mountain Newt, *Neurergus derjugini* (Caudata, Salamandridae). *Journal of Zoological Systematics and Evolutionary Research* **57:** 580–590.

Aiello-Lammens ME, **Boria RA**, **Radosavljević A**, **Vilela B**, **Anderson RP. 2015.** spThin: an R package for spatial thinning of species occurrence records for use in ecological niche models. *Ecography* **38:** 541–545.

Anselin L, **Syabri I**, **Kho Y 2006.** *GeoDa*: an introduction to spatial data analysis. *Geographical Analysis* **38:** 5–22.

Arnold NE, **Arribas O**, **Carranza S. 2007.** Systematics of the Palaearctic and Oriental lizard tribe Lacertini (Squamata: Lacertidae: Lacertinae), with description of eight new genera. *Zootaxa* **1430:** 1–86.

Asimakopoulos B. 1994. A morphometric comparison between Green and Italian samples of *Rana graeca* (Amphibia, Anura). *Bios* **2:** 87–89.

Asimakopoulos B, **Grossenbacher K. 2014.** *Rana graeca* Boulenger, 1891 – Griechischer Frosch. In: Böhme W, ed. *Handbuch der Reptilien und Amphibien Europas. Band 5 / IIIA: Froschlurche (Anura) IIIA (Ranidae I)*. Wiebelsheim: AULA-Verlag, 187–203.

Babik W, **Branicki W**, **Sandera M**, **Litvinchuk S**, **Borkin LJ**, **Irwin JT**, **Rafiński J. 2004.** Mitochondrial phylogeography of the moor frog, *Rana arvalis*. *Molecular Ecology* **13:** 1469–1480.

Boria RA, **Olson LE**, **Goodman SM**, **Anderson RP 2014.** Spatial filtering to reduce sampling bias can improve the performance of ecological niche models. *Ecological Modelling* **275:** 73–77.

Bouckaert RR, **Drummond AJ. 2017.** bModelTest: Bayesian phylogenetic site model averaging and model comparison. *BMC Evolutionary Biology* **17:** 42.

Bouckaert RR, **Vaughan TG**, **Barido-Sottani J**, **Duchêne S**, **Fourment M**, **Gavryushkina A**, **Heled J**, **Jones G**, **Kühnert D**, **De Maio N**, **Matschiner M**, **Mendes FK**, **Müller NF**, **Ogilvie HA**, **du Plessis L**, **Popinga A**, **Rambaut A**, **Rasmussen D**, **Siveroni I**, **Suchard MA**, **Wu CH**, **Xie D**, **Zhang C**, **Stadler T**, **Drummond AJ. 2019.** BEAST 2.5: an advanced software platform for Bayesian evolutionary analysis. *PLoS Computational Biology* **15:** e1006650.

Bringsøe H. 2011. Possible circadian colour change in *Rana graeca* in Albania. *Zeitschrift für Feldherpetologie* **18:** 93–98.

Brown JL, **Hill DJ**, **Dolan AM**, **Carnaval AC**, **Haywood AM. 2018.** PaleoClim, high spatial resolution paleoclimate surfaces for global land areas. *Scientific Data* **5:** 180254.

Bruford MW, **Hanotte O**, **Burke T. 1998.** Multi and single locus DNA fingerprinting. In: Hoelzel AR, ed., *Molecular genetic analysis of populations: a practical approach*. Oxford: IRL Press, 225–269.

Canestrelli D, **Bisconti R**, **Sacco F**, **Nascetti G. 2014.** What triggers the rising of an intraspecific biodiversity hotspot? Hints from the agile frog. *Scientific Reports* **4:** 5042.

Canestrelli D, **Cimmaruta R**, **Nascetti G. 2008.** Population genetic structure and diversity of the Apennine endemic stream frog, *Rana italica* – insights on the Pleistocene evolutionary history of the Italian peninsular biota. *Molecular Ecology* **17:** 3856–3872.

Carranza S, **Arribas, O. 2008.** Genetic uniformity of *Rana pyrenaica* Serra-Cobo, 1993 across its distribution range: a preliminary study with mtDNA sequences. *Amphibia-Reptilia* **29:** 579–582.

Dermitzakis DM. 1990. The colonisation of Aegean islands in relation with the paleogeographic evolution. *Biologia Gallo – Hellenica* **17:** 99–130.

Dormann CF, **Elith J**, **Bacher S**, **Buchmann C**, **Carl G**, **Carré G**, **Marquéz, JRG**, **Gruber B**, **Lafourcade B**, **Leitão PJ**, **Münkemüller T**, **McClean C**, **Osborne PE**, **Reineking B**, **Schröder B**, **Skidmore AK**, **Zurell D**, **Lautenbach S 2013.** Collinearity: a review of methods to deal with it and a simulation study evaluating their performance. *Ecography* **36:** 27–46.

Drummond AJ, **Rambaut A**, **Shapiro B**, **Pybus OG. 2005.** Bayesian coalescent inference of past population dynamics from molecular sequences. *Molecular Biology and Evolution* **22:** 1185–1192.

Dufresnes C, **Mazepa G**, **Jablonski D**, **Oliveira RC**, **Wenseleers T**, **Shabanov DA**, **Auer M**, **Ernst R**, **Koch C**, **Ramírez-Chaves HE**, **Mulder KP**, **Simonov E**, **Tiutenko A**, **Kryvokhyzha D**, **Wennekes PL**, **Zinenko OI**, **Korshunov OV**, **Al-Johany AM**, **Peregontsev EA**, **Masroor R**, **Betto-Colliard C**, **Denoël M**, **Borkin LJ**, **Skorinov DV**, **Pasynkova RA**, **Mazanaeva LF**, **Rosanov JM**, **Dubey S**, **Litvinchuk S. 2019a.** Fifteen shades of green: the evolution of *Bufotes* toads revisited. *Molecular Phylogenetics and Evolution* **141:** 106615.

Dufresnes C, **Mazepa G**, **Rodrigues N**, **Brelsford A**, **Litvinchuk SN**, **Sermier R**, **Lavanchy G**, **Betto-Colliard C**, **Blaser O**, **Borzée A**, **Cavoto E**, **Fabre G**, **Ghali K**, **Grossen C**, **Horn A**, **Leuenberger J**, **Phillips BC**, **Saunders PA**, **Savary R**, **Maddalena T**, **Stöck M**, **Dubey S**, **Canestrelli D**, **Jeffries DL. 2018.** Genomic evidence for cryptic speciation in tree frogs from the Apennine Peninsula, with description of *Hyla perrini* sp. nov. *Frontiers in Ecology and Evolution* **6:** 144.

Dufresnes C, **Nicieza AG**, **Litvinchuk SN**, **Rodrigues N**, **Jeffries DL**, **Vences M**, **Perrin N**, **Martínez-Solano Í. 2020.** Are glacial refugia hotspots of speciation and cytonuclear discordances? Answers from the genomic phylogeography of Spanish common frogs. *Molecular Ecology* **29:** 986–1000.

Dufresnes C, **Strachinis I**, **Suriadna N**, **Mykytynets G**, **Cogălniceanu D**, **Székely P**, **Vukov T**, **Arntzen JW**, **Wielstra B**, **Lymberakis P**, **Geffen E**, **Gafny S**, **Kumlutaş Y**, **Ilgaz Ç**, **Candan K**, **Mizsei E**, **Szabolcs M**, **Kolenda K**, **Smirnov N**, **Géniez P**, **Lukanov S**, **Crochet PA**, **Dubey S**, **Perrin N**, **Litvinchuk SN**, **Denoël M. 2019b.** Phylogeography of a cryptic speciation continuum in Eurasian spadefoot toads (*Pelobates*). *Molecular Ecology* **28:** 3257–3270.

Dufresnes C, **Wassef J**, **Ghali K**, **Brelsford A**, **Stöck M**, **Lymberakis P**, **Crnobrnja-Isailovic J**, **Perrin N. 2013.** Conservation phylogeography: does historical diversity contribute to regional vulnerability in European tree frogs (*Hyla arborea*)? *Molecular Ecology* **22:** 5669–5684.

Environmental Systems Research Institute. **2019.** *ArcGIS release 10.5*. Redlands.

Fijarczyk A, **Nadachowska K**, **Hofman S**, **Litvinchuk SN**, **Babik W**, **Stuglik M**, **Gollmann G**, **Choleva L**, **Cogălniceanu D**, **Vukov T**, **Džukić G**, **Szymura JM. 2011.** Nuclear and mitochondrial phylogeography of the European fire-bellied toads *Bombina bombina* and *Bombina variegata* supports their independent histories. *Molecular Ecology* **20:** 3381–3398.

Fordham DA, **Saltré F**, **Haythorne S**, **Wigley TML**, **Otto-Bliesner BL**, **Chan KC**, **Brook B. 2017.** PaleoView: a tool for generating continuous climate projections spanning the last 21 000 years at regional and global scales. *Ecography* **40:** 1348–1358.

Fu YX. 1997. Statistical tests of neutrality of mutations against population growth, hitchhiking and background selection. *Genetics* **147:** 915–925.

GBIF. **2020.** *Rana graeca Boulenger, 1891 in GBIF Secretariat. GBIF Backbone Taxonomy*. Checklist dataset. Available at: https://doi.org/10.15468/39omei

Griffiths HI, **Kryštufek B**, **Reed JM. 2004.** *Balkan biodiversity. Pattern and process in the European hotspot*. Amsterdam: Springer.

Guindon S, **Dufayard JF**, **Lefort V**, **Anisimova M**, **Hordijk W**, **Gascuel O. 2010.** New algorithms and methods to estimate maximum-likelihood phylogenies: assessing the performance of PhyML 3.0. *Systematic Biology* **59:** 307–321.

Hao T, **Elith J**, **Lahoz-Monfort JJ**, **Guillera-Arroita G. 2020.** Testing whether ensemble modelling is advantageous for maximising predictive performance of species distribution models. *Ecography* **43:** 549–558.

Hewitt GM. 2011. Mediterranean peninsulas: the evolution of hotspots. In: Zachos FE, Habel JC, eds. *Biodiversity Hotspots*. Berlin, Heidelberg: Springer, 123–147.

Huelsenbeck JP, **Ronquist F. 2001.** MRBAYES: Bayesian inference of phylogenetic trees. *Bioinformatics* **17:** 754–755.

Ilić M, **Stamenković G**, **Nikolić V**, **Markovi V**, **Marinković N**, **Paunović M**, **Crnobrnja-Isailović J. 2016.** Identification of syntopic anuran species in early tadpole stages: correspondence between morphometric and genetic data. *Applied Ecology and Environmental Research* **14:** 381–397.

Jablonski D, **Jandzik D**, **Mikulíček P**, **Džukić G**, **Ljubisavljević K**, **Tzankov N**, **Jelić D**, **Thanou E**, **Moravec J**, **Gvoždík V. 2016.** Contrasting evolutionary histories of the legless lizards slow worms (*Anguis*) shaped by the topography of the Balkan Peninsula. *BMC Evolutionary Biology* **16:** 99.

Jablonski D, **Nagy ZT**, **Avcı A**, **Olgun K**, **Kukushkin OV**, **Safaei-Mahroo B**, **Jandzik D. 2019.** Cryptic diversity in the smooth snake (*Coronella austriaca*). *Amphibia-Reptilia* **40:** 179–192.

Johnson KP, **Sorenson MD. 1998.** Comparing molecular evolution in two mitochondrial protein coding genes (cytochrome *b* and ND2) in the dabbling ducks (Tribe: Anatini). *Molecular Phylogenetics and Evolution* **10:** 82–94.

Kapli P, **Botoni D**, **Ilgaz C**, **Kumlutaş Y**, **Avcı A**, **Rastegar-Pouyani N**, **Fathinia B**, **Lymberakis P**, **Ahmadzadeh F**, **Poulakakis N. 2013.** Molecular phylogeny and historical biogeography of the Anatolian lizard *Apathya* (Squamata, Lacertidae). *Molecular Phylogenetics and Evolution* **66:** 992–1001.

Karger DN, **Conrad O**, **Böhner J**, **Kawohl T**, **Kreft H**, **Soria-Auza RW**, **Zimmermann NE**, **Linder HP**, **Kessler M.**

2017. Climatologies at high resolution for the Earth's land surface areas. *Scientific Data* **4:** 170122.

Kass JM, **Vilela B**, **Aiello-Lammens ME**, **Muscarella R**, **Merow C**, **Anderson RP. 2018.** WALLACE: A flexible platform for reproducible modeling of species niches and distributions built for community expansion. *Methods in Ecology and Evolution* **9:** 1151–1156.

Kindler C, **Graciá E**, **Fritz U. 2018.** Extra-Mediterranean glacial refuges in barred and common grass snake (Natrix helvetica, N. natrix). *Scientific Reports* **8:** 182.

Kotsakiozi P, **Jablonski D**, **Ilgaz Ç**, **Kumlutaş Y**, **Avcı A**, **Meiri S**, **Itescu Y**, **Kukushkin O**, **Gvoždík V**, **Scillitani G**, **Roussos SA**, **Jandzik D**, **Kasapidis P**, **Lymberakis P**, **Poulakakis N. 2018.** Multilocus phylogeny and coalescent species delimitation in Kotschy's gecko, *Mediodactylus kotschyi*: hidden diversity and cryptic species. *Molecular Phylogenetics and Evolution* **125:** 177–187.

Kryštufek B, **Bužan EV**, **Hutchinson WF**, **Hanfling B. 2007.** Phylogeography of the rare Balkan endemic Martino's vole, *Dinaromys bogdanovi*, reveals strong differentiation within the western Balkan Peninsula. *Molecular Ecology* **16:** 1221–1232.

Kumar S, **Stecher G**, **Li M**, **Knyaz C**, **Tamura K. 2018.** MEGA X: molecular evolutionary genetics analysis across computing platforms. *Molecular Biology and Evolution* **35:** 1547–1549.

Lanfear R, **Frandsen PB**, **Wright AM**, **Senfeld T**, **Calcott B. 2017.** PartitionFinder 2: new methods for selecting partitioned models of evolution for molecular and morphological phylogenetic analyses. *Molecular Biology and Evolution* **34:** 772–773.

Lymberakis P, **Poulakakis N**, **Manthalou G**, **Tsigenopoulos CS**, **Magoulas A**, **Mylonas M. 2007.** Mitochondrial phylogeography of *Rana* (*Pelophylax*) populations in the Eastern Mediterranean region. *Molecular Phylogenetics and Evolution* **44:** 115–125.

Marzahn E, **Mayer W**, **Joger U**, **Ilgaz Ç**, **Jablonski D**, **Kindler C**, **Kumlutaş Y**, **Nistri A**, **Schneeweiß N**, **Vamberger M**, **Žagar A**, **Fritz U. 2016.** Phylogeography of the *Lacerta viridis* complex: mitochondrial and nuclear markers provide taxonomic insights. *Journal of Zoological Systematics and Evolutionary Research* **54:** 85–105.

Meulenkamp JE 1985. Aspects of the late Cenozoic evolution of the aegean region. In: Stanley DJ, Wezel FC, eds. *Geological evolution of the Mediterranean basin*. New York: Springer, 307–321.

Mizsei E, **Jablonski D**, **Roussos SA**, **Dimaki M**, **Ioannidis Y**, **Nilson G**, **Nagy ZT. 2017.** Nuclear markers support the mitochondrial phylogeny of *Vipera ursinii–renardi* complex (Squamata: Viperidae) and species status for the Greek meadow viper. *Zootaxa* **4227:** zootaxa.4227.1.4.

Morales NS, **Fernández IC**, **Baca-González V. 2017.** MaxEnt's parameter configuration and small samples: are we paying attention to recommendations? A systematic review. *PeerJ* **5:** e3093.

Muscarella R, **Galante PJ**, **Soley-Guardia M**, **Boria RA**, **Kass JM**, **Uriarte M**, **Anderson RP. 2014.** ENMeval: an R package for conducting spatially independent evaluations and estimating optimal model complexity for MAXENT ecological niche models. *Methods in Ecology and Evolution* **5:** 1198–1205.

Nagy ZT, **Schmidtler JF**, **Joger U**, **Wink M. 2003.** Systematik der Zwergnattern (Reptilia: Colubridae: *Eirenis*) und verwandter Gruppen anhand von DNA-Sequenzen und morphologishech Daten. *Salamandra* **39:** 149–168.

Naimi B, **Hamm NAS**, **Groen TA**, **Skidmore AK**, **Toxopeus AG. 2014.** Where is positional uncertainty a problem for species distribution modelling? *Ecography* **37:** 191–203.

Pabijan M, **Zieliński P**, **Dudek K**, **Chloupek M**, **Sotiropoulos K**, **Liana M**, **Babik W. 2015.** The dissection of a Pleistocene refugium: phylogeography of the smooth newt, *Lissotriton vulgaris*, in the Balkans. *Journal of Biogeography* **42:** 671–683.

Picariello O, **Feliciello I**, **Bellinello R**, **Chinali G. 2002.** S1 satellite DNA as a taxonomic marker in brown frogs: molecular evidence that *Rana graeca graeca* and *Rana graeca italica* are different species. *Genome* **45:** 63–70.

Podnar M, **Mađarić BB**, **Mayer W. 2014.** Non-concordant phylogeographical patterns of three widely codistributed endemic Western Balkans lacertid lizards (Reptilia, Lacertidae) shaped by specific habitat requirements and different responses to Pleistocene climatic oscillations. *Journal of Zoological Systematics and Evolutionary Research* **52:** 119–129.

Posada D, **Crandall KA. 2001.** Intraspecific gene genealogies: trees grafting into networks. *Trends in Ecology & Evolution* **16:** 37–45.

Poulakakis N, **Kapli P**, **Kardamaki A**, **Skourtanioti E**, **Göçmen B**, **Ilgaz C**, **Kumlutas Y**, **Avci A**, **Lymberakis P. 2013.** Comparative phylogeography of six herpetofauna species in Cyprus: late Miocene to Pleistocene colonization routes. *Biological Journal of the Linnean Society* **108:** 619–635.

Poulakakis N, **Kapli P**, **Lymberakis P**, **Trichas A**, **Vardinoyiannis K**, **Sfenthourakis S**, **Mylonas M. 2015.** A review of phylogeographic analyses of animal taxa from the Aegean and surrounding regions. *Journal of Zoological Systematics and Evolutionary Research* **53:** 18–32.

Psonis N, **Antoniou A**, **Karameta E**, **Leaché AD**, **Kotsakiozi P**, **Darriba D**, **Kozlov A**, **Stamatakis A**, **Poursanidis D**, **Kukushkin O**, **Jablonski D**, **Crnobrnja-Isailović J**, **Gherghel I**, **Lymberakis P**, **Poulakakis N. 2018.** Resolving complex phylogeographic patterns in the Balkan Peninsula using closely related wall-lizard species as a model system. *Molecular Phylogenetics and Evolution* **125:** 100–115.

Psonis N, **Antoniou A**, **Kukushkin O**, **Jablonski D**, **Petrov B**, **Crnobrnja-Isailović J**, **Sotiropoulos K**, **Gherghel I**, **Lymberakis P**, **Poulakakis N. 2017.** Hidden diversity in the *Podarcis tauricus* (Sauria, Lacertidae) species subgroup in the light of multilocus phylogeny and species delimitation. *Molecular Phylogenetics and Evolution* **106:** 6–17.

QGIS Development Team. **2020.** *QGIS geographic information system. Open source geospatial foundation project*. Available at: http://qgis.osgeo.org

R Core Team. **2020.** *R: a language and environment for statistical computing*. Vienna: R Foundation for Statistical Computing. Available at: https://www.R-project.org/

Radosavljević A, **Anderson RP. 2014.** Making better MAXENT models of species distributions: complexity, overfitting and evaluation. *Journal of Biogeography* **41:** 629–643.

Rambaut A, **Suchard MA**, **Xie D**, **Drummon AJ. 2014.** *Tracer v1.6*. Available at: http://beast.bio.ed.ac.uk/Tracer

Recuero E, **Buckley D**, **García-París M**, **Arntzen JW**, **Cogălniceanu D**, **Martínez-Solano I. 2014.** Evolutionary history of *Ichthyosaura alpestris* (Caudata, Salamandridae) inferred from the combined analysis of nuclear and mitochondrial markers. *Molecular Phylogenetics and Evolution* **81:** 207–220.

Recuero E, **García-París M. 2011.** Evolutionary history of *Lissotriton helveticus*: multilocus assessment of ancestral vs. recent colonization of the Iberian Peninsula. *Molecular Phylogenetics and Evolution* **60:** 170–182.

Ronquist F, **Teslenko M**, **van der Mark P**, **Ayres DL**, **Darling A**, **Höhna S**, **Larget B**, **Liu L**, **Suchard MA**, **Huelsenbeck JP. 2012.** MrBayes 3.2: efficient Bayesian phylogenetic inference and model choice across a large model space. *Systematic Biology* **61:** 539–542.

Rozas J, **Ferrer-Mata A**, **Sánchez-DelBarrio JC**, **Guirao-Rico S**, **Librado P**, **Ramos-Onsins SE**, **Sánchez-Gracia A. 2017.** DnaSP 6: DNA sequence polymorphism analysis of large data sets. *Molecular Biology and Evolution* **34:** 3299–3302.

Salvi D, **Harris DJ**, **Kaliontzopoulou A**, **Carretero MA**, **Pinho C. 2013.** Persistence across Pleistocene ice ages in Mediterranean and extra-Mediterranean refugia: phylogeographic insights from the common wall lizard. *BMC Evolutionary Biology* **13:** 147.

Schmitt T, **Varga Z. 2012.** Extra-Mediterranean refugia: the rule and not the exception? *Frontiers in Zoology* **9:** 22.

Sillero N, **Campos J**, **Bonardi A**, **Corti C**, **Creemers R**, **Crochet P-A**, **Crnobrnja Isailovic J**, **Denoël M**, **Ficetola GF**, **Gonçalves J**, **Kuzmin S**, **Lymberakis P**, **de Pous P**, **Rodríguez A**, **Sindaco R**, **Speybroeck J**, **Toxopeus B**, **Vieites DR**, **Vences M. 2014.** Updated distribution and biogeography of amphibians and reptiles of Europe. *Amphibia-Reptilia* **35:** 1–31.

Silvestro D, **Michalak I. 2011.** raxmlGUI: a graphical front-end for RAxML. *Organisms Diversity & Evolution* **12:** 335–337.

Slatkin M, **Excoffier L. 2012.** Serial founder effects during range expansion: a spatial analog of genetic drift. *Genetics* **191:** 171–181.

Speybroeck J, **Beukema W**, **Bok B**, **Van Der Voort J**, **Velikov I. 2016**. *Field guide to the amphibians and reptiles of Britain and Europe*. London: Bloomsbury Publishing.

Spilani L, **Bougiouri K**, **Antoniou A**, **Psonis N**, **Poursanidis D**, **Lymberakis P**, **Poulakakis N. 2019.** Multigene phylogeny, phylogeography and population structure of *Podarcis cretensis* species group in south Balkans. *Molecular Phylogenetics and Evolution* **138:** 193–204.

Stewart JR, **Lister AM**, **Barnes I**, **Dalén L. 2010.** Refugia revisited: individualistic responses of species in space and time. *Proceedings of the Royal Society B: Biological Sciences* **277:** 661–671.

Stojanov A, **Tzankov N**, **Naumov B. 2011.** *Die amphibien und reptilien Bulgariens*. Frankfurt am Main: Edition Chimaira.

Šukalo G, **Dmitrović D**, **Filipović S**, **Kovačević M**, **Dordjević S**, **Tomović L. 2015.** New findings of the Greek frog, *Rana graeca* Boulenger, 1891 (Anura: Ranidae) in the north-western Bosnia and Herzegovina. *Ecologica Montenegrina* **2:** 74–77.

Šunje E, **Jelić D**, **Vörös J. 2018.** Insights into the phylogeny and phylogeography of the frog *Rana graeca* in the Balkan Peninsula (Amphibia: Anura). *Salamandra* **54:** 278–282.

Šunje E, **Lelo S**, **Jelić D. 2017.** Revizija distribucije i statusa ugroženosti Potočne žabe (*Rana graeca* Boulenger, 1891) u Bosne i Hercegovini. *Prilozi fauni Bosne i Hercegovine* **13:** 87–100.

Szabolcs M, **Mizsei E**, **Jablonski D**, **Vági B**, **Mester B**, **Végvári Z**, **Lengyel S. 2017.** Distribution and diversity of amphibians in Albania: new data and basis for a comprehensive database. *Amphibia-Reptilia* **38:** 435–448.

Tajima F. 1989. Statistical method for testing the neutral mutation hypothesis by DNA polymorphism. *Genetics* **123:** 585–595.

Teixeira J, **Gonçalves H**, **Ferrand N**, **García-París M**, **Recuero E. 2018.** Mitochondrial phylogeography of the Iberian endemic frog *Rana iberica*, with implications for its conservation. *Current Zoology* **64:** 755–764.

Ueda K. 2020. *iNaturalist research-grade observations. iNaturalist.org*. Occurrence dataset. Available at: https://doi.org/10.15468/ab3s5x

Valakos E, **Pafilis P**, **Sotiropoulos K**, **Lymberakis P**, **Maragou P**, **Foufopoulos J. 2008.** *The amphibians and reptiles of Greece.* Frankfurt am Main: Edition Chimaira.

Veith M, **Kosuch J**, **Vences M. 2003.** Climatic oscillations triggered post-Messinian speciation of Western Palearctic brown frogs (Amphibia, Ranidae). *Molecular Phylogenetics and Evolution* **26:** 310–327.

Vences M, **Hauswaldt JS**, **Steinfartz S**, **Rupp O**, **Goesmann A**, **Künzel S**, **Orozco-terWengel P**, **Vieites DR**, **Nieto-Roman S**, **Haas S**, **Laugsch C**, **Gehara M**, **Bruchmann S**, **Pabijan M**, **Ludewig AK**, **Rudert D**, **Angelini C**, **Borkin LJ**, **Crochet PA**, **Crottini A**, **Dubois A**, **Ficetola GF**, **Galán P**, **Geniez P**, **Hachtel M**, **Jovanovic O**, **Litvinchuk SN**, **Lymberakis P**, **Ohler A**, **Smirnov NA. 2013.** Radically different phylogeographies and patterns of genetic variation in two European brown frogs, genus *Rana*. *Molecular Phylogenetics and Evolution* **68:** 657–670.

Vucić M, **Jelić D**, **Klobučar GIV**, **Prkljačić B**, **Jelić M. 2018.** Molecular identification of species and hybrids of water frogs (genus *Pelophylax*) from Lake Skadar, Southeast Adriatic drainages (Amphibia: Ranidae). *Salamandra* **54:** 147–157.

Warren DL, **Seifert SN. 2011.** Ecological niche modeling in Maxent: the importance of model complexity and the performance of model selection criteria. *Ecological Applications* **21:** 335–342.

Wielstra B, **Canestrelli D**, **Cvijanović M**, **Denoël M**, **Fijarczyk A**, **Jablonski D**, **Liana M**, **Naumov B**, **Olgun KB**,

Pabijan M, **Pezzarossa A**, **Popgeorgiev G**, **Salvi D**, **Si Y**, **Sillero N**, **Sotiropoulos K**, **Zieliński P**, **Babik W. 2018.** The distributions of the six species constituting the smooth newt species complex (*Lissotriton vulgaris* sensu lato and *L. montandoni*) – an addition to the New Atlas of Amphibians and Reptiles of Europe. *Amphibia-Reptilia* **39:** 252–259.

Wielstra B, **Crnobrnja-Isailović J**, **Litvinchuk SN**, **Reijnen BT**, **Skidmore AK**, **Sotiropoulos K**, **Toxopeus AG**, **Tzankov N**, **Vukov T**, **Arntzen JW. 2013.** Tracing glacial refugia of *Triturus* newts based on mitochondrial DNA phylogeography and species distribution modeling. *Frontiers in Zoology* **10:** 13.

Wielstra B, **Sillero N**, **Vörös J**, **Arntzen JW. 2014.** The distribution of the crested and marbled newt species (Amphibia: Salamandridae: *Triturus*) – an addition to the New Atlas of Amphibians and Reptiles of Europe. *Amphibia-Reptilia* **35:** 376–381.

Yang Z. 2006. *Computational molecular evolution*. Oxford, New York: Oxford University Press.

Yuan ZY, **Zhou WW**, **Chen X**, **Poyarkov NA Jr**, **Chen HM**, **Jang-Liaw NH**, **Chou WH**, **Matzke NJ**, **Iizuka K**, **Min MS**, **Kuzmin SL**, **Zhang YP**, **Cannatella DC**, **Hillis DM**, **Che J. 2016.** Spatiotemporal diversification of the true frogs (genus *Rana*): a historical framework for a widely studied group of model organisms. *Systematic Biology* **65:** 824–842.

Zhang D. 2020. *rsq: R-squared and related measures*. Available at: https://cran.r-project.org/web/packages/rsq/index.html

SUPPORTING INFORMATION

Additional Supporting Information may be found in the online version of this article at the publisher's web-site:

Table S1. List of samples and sequences used for analyses.
Table S2. Primers and conditions used in polymerase chain reaction amplifications and in cycle sequencing reactions.
Table S3. Partitioning schemes and best-fitting models of sequence evolution selected in PARTITIONFINDER (PF) for downstream analyses.
Table S4. Complete occurrence data for species distribution modelling.
Table S5. Selected and partitioned data for species distribution modelling.
Table S6. Eight main variables forming the species distribution modelling of the species.
Table S7. GenBank numbers of sequences used for DNA polymorphism of endemic species.
Table S8. Overview of DNA polymorphism and genetic diversity of all species of amphibians and reptiles endemic in the continental Balkans, based on mitochondrial DNA, and their species ranges (in square kilometres). Abbreviations: h, number of haplotypes; h_d, haplotype diversity; N, number of species; π, nucleotide diversity. *The source with an estimated time of divergence.
Figure S1. The area of work, covering almost the whole of the Balkan Peninsula. Using coloured dots, the occurrence data of the Greek frog (*Rana graeca*) are split using the block method.
Figure S2. Phylogenetic relationships of *Rana* reconstructed using Bayesian inference of 16S, *Cytb* and *COI* sequences. The numbers above the branches represent Bayesian posterior probabilities showing the branch support. For details, see the Supporting Information (Table S1).
Figure S3. Phylogenetic relationships of *Rana* reconstructed using maximum likelihood of 16S, *Cytb* and *COI* sequences. The numbers above the branches represent bootstraps showing the branch support. For details, see the Supporting Information (Table S1).
Figure S4. Phylogenetic relationships of *Rana* reconstructed using Bayesian inference of 16S and *Cytb* sequences. The numbers above the branches represent Bayesian posterior probabilities showing the branch support. For details, see the Supporting Information (Table S1).
Figure S5. Phylogenetic relationships of *Rana* reconstructed using maximum likelihood of 16S and *Cytb* sequences. The numbers above the branches represent bootstraps showing the branch support. For details, see the Supporting Information (Table S1).
Figure S6. Phylogenetic relationships of *Rana* reconstructed using Bayesian inference of *BDNF* sequences. The numbers above the branches represent Bayesian posterior probabilities showing the branch support. For details, the Supporting Information (Table S1).
Figure S7. Phylogenetic relationships of *Rana* reconstructed using maximum likelihood of *BDNF* sequences. The numbers above the branches represent bootstraps showing the branch support. For details, see the Supporting Information (Table S1).